NMR Analysis of Interacting Soluble Forms of the Cell−Cell Recognition Molecules CD2 and CD48†

Mark S. B. McAlister,[‡,§] Helen R. Mott,[‡,||] P. Anton van der Merwe,[⊥] Iain D. Campbell,[‡] Simon J. Davis,[⊥,#] and Paul C. Driscoll*[,‡,§]

Department of Biochemistry, University of Oxford, South Parks Road, Oxford OX1 3QU, U.K., and MRC Cellular Immunology Unit, Sir William Dunn School of Pathology, University of Oxford, Oxford OX1 3RE, U.K.

Received November 20, 1995; Revised Manuscript Received February 21, 1996[⊗]

ABSTRACT: The T cell glycoprotein, CD2, is one of the best characterized molecules mediating recognition at the cell surface. The ligands of murine and human CD2 are CD48 and CD58, respectively, and interactions between these molecules have been shown to influence antigen recognition and T cell activation. The CD58 binding site of human CD2 has been characterized in mutational studies, and here we use heteronuclear NMR spectroscopy to identify the rat CD48 binding site of the N-terminal domain of rat CD2 (CD2d1). The NMR spectrum of bacterially expressed CD2d1, assigned initially at pH 4.3 in the course of determining the three-dimensional solution structure of this domain [Driscoll, P. C., et al. (1991) *Nature 353*, 762−765], has been reassigned as a two-dimensional $^{15}N-^{1}H$ heteronuclear single-quantum coherence (HSQC) spectrum at neutral pH. The CD48 binding surface was identified by monitoring perturbations in the line widths and chemical shifts of cross peaks in the HSQC spectrum of CD2d1 during titrations with a soluble form of CD48 expressed in Chinese hamster ovary cells. This first solution NMR analysis of interacting cell surface molecules shows that the ligand binding site extends across an area of *ca.* 700−800 Å^2 of the GFCC′C″ face corresponding almost exactly to lattice contacts in crystals of soluble CD2 first proposed as a model of the interaction of CD2 with its ligands. The analysis finds no evidence for any large-scale structural changes in domain 1 of CD2 to accompany CD48 binding. Comparisons of the human and rat CD2 ligand binding sites suggest that species- and ligand-specific binding may be determined by as few as three amino acid residues, corresponding to Thr37, Leu38, and Glu41 in rat CD2 (Lys42, Lys43, and Gln46 in human CD2).

The T cell glycoprotein, CD2, was the first molecule shown to be involved in heterophilic cell−cell recognition (Hunig, 1985). A role in cell−cell recognition was first implied by the ability of anti-CD2 antibodies to block the interaction of human T cells with sheep red blood cells [reviewed by Bierer et al. (1989), Moingeon et al. (1989), and Dustin and Springer (1991)]. It is now clear that the physiological counterparts of this interaction, which involve the binding of CD2 to CD58 in humans (Selvaraj et al., 1987) and to CD48 in mice and rats (Kato et al., 1992; van der Merwe et al., 1993a), can augment T cell responses [reviewed by Bierer et al. (1989), Moingeon et al. (1989), and Dustin and Springer (1991)]. In addition to mediating cell−cell recognition, CD2 appears to be linked to T cell activation pathways since certain pairs of monoclonal antibodies are mitogenic for human (Meuer et al., 1984) and rat T cells (Clark et al., 1988). However, CD2 is part of a multimolecular complex which includes the T cell receptor, CD3, CD4 (or CD8), and CD5 (Beyers et al., 1992), and it is known that T cell activation via CD2 is entirely dependent on the presence of the T cell receptor (Spruyt et al., 1991). Therefore, it is not certain that signaling through CD2 *per se*, if it occurs at all *in vivo*, is physiologically important. The unusual effects of certain activating anti-CD2 antibodies suggested that conformational changes could mediate some of the physiological functions of the molecule (Meuer et al., 1984). While antibodies are unlikely to exert their effects in this way (Davis et al., 1995a), the possibility that ligand binding induces such changes has not been addressed.

The three-dimensional solution structures of the membrane distal domains of rat CD2 (CD2d1)[1] (Driscoll et al., 1991) and human CD2 (Withka et al., 1993) were determined by NMR spectroscopy, confirming the prediction that CD2 belongs to the immunoglobulin superfamily (Williams et al., 1987). Crystallographic studies (Jones et al., 1992; Bodian et al., 1994) showed that the extracellular portion of CD2 consists of two immunoglobulin-like domains: a membrane proximal C2-set domain and a membrane distal V-set domain which lacks the consensus disulfide bond (Driscoll et al.,

† This work was performed under the auspices of the Oxford Centre for Molecular Sciences, which is funded by the BBSRC and the MRC. Grant support for M.S.B.M. and S.J.D. came from the Human Frontier Science Program Organisation. P.C.D. is a Royal Society University Research Fellow.

* To whom correspondence should be addressed.

‡ Department of Biochemistry, University of Oxford.

§ Current address: Department of Biochemistry and Molecular Biology, University College London, Gower St., London WC1E 6BT, U.K.

|| Current address: Department of Biochemistry and Biophysics, University of North Carolina, CB #7260, Chapel Hill, NC 27599.

⊥ MRC Cellular Immunology Unit, Sir William Dunn School of Pathology, University of Oxford.

Current address: Molecular Science Division, Nuffield Department of Clinical Medicine, University of Oxford, John Radcliffe Hospital, Oxford OX3 9DU, U.K.

⊗ Abstract published in *Advance ACS Abstracts,* April 1, 1996.

[1] Abbreviations: CD2d1, N-terminal domain of rat CD2 (residues 1−99); sCD48, soluble form of rat CD48 consisting of the entire extracellular region; sCD2, soluble form of CD2 consisting of the entire extracellular region; NMR, nuclear magnetic resonance; NOESY, nuclear Overhauser effect spectroscopy; HSQC, heteronuclear single-quantum correlation; CHO, Chinese hamster ovary.

S0006-2960(95)02756-5 CCC: $12.00

1991). The sequences and chromosomal locations of the genes encoding CD2, CD48, and CD58 suggest that these proteins have very similar structures and that the genes may have evolved by duplication from an ancestor encoding a protein involved in homophilic recognition (Killeen et al., 1988; Wong et al., 1990).

The monomeric binding affinities of rat CD2 and CD48 (van der Merwe et al., 1993b) and of human CD2 and CD58 (van der Merwe et al., 1994) are low with dissociation constant (K_d) values of 60−90 and 9−22 μM, respectively. In both cases the binding is characterized by a fast on-rate and a very fast off-rate that may allow transient, reversible cell−cell interactions. The ligand interactions of CD2 appear to be glycosylation independent (van der Merwe et al., 1993a; Davis et al., 1995b), but this is controversial (Recny et al., 1992; Wyss et al., 1995). Mutational studies of CD58 binding by human CD2 (Somoza et al., 1993; Arulanandam et al., 1993) implicate the major β-sheet surface of domain 1, which consists of β-strands labeled G,F,C,C′ and C″ (using the standard description of the topology of immunoglobulin superfamily domains; Williams & Barclay, 1988; Bork et al., 1994). As a protein−protein binding site the GFCC′C″ face of CD2 has two unusual features (Bodian et al., 1994). First, it is much flatter than other protein binding sites, suggesting that the CD2−ligand interface has less surface complementarity. Second, the GFCC′C″ face has a larger proportion of polar or charged residues than other sites of protein recognition: 70−90% of the residues in the GFC-C′C″ face of CD2 are polar or charged whereas less than 50% of the residues forming the binding sites of antibodies and proteases have these properties. The preponderance of charged residues in the binding face suggests that electrostatic complementarity at the CD2−ligand interface contributes significantly to binding specificity.

Consistent with the possibility that CD2, CD48, and CD58 all evolved from a homophilic precursor, mutational studies of CD58 (Arulanandam et al., 1994) and rat CD48 (van der Merwe et al., 1995) indicate that, like CD2, the GFCC′C″ faces of the N-terminal domains of these molecules are also used for ligand binding. In the crystals of both rat and human soluble CD2 (sCD2) very similar, extensive lattice contacts are observed that involve the domain 1 GFCC′C″ β-sheets of all the molecules in each asymmetric unit (Jones et al., 1992; Bodian et al., 1994). There is little evidence that CD2 self-associates under physiological conditions (van der Merwe et al., 1993c). However, it was proposed that this crystal contact, which is comparable to the standard orthogonal mode of β-sheet packing, represents a plausible model for heterophilic ligand recognition by CD2, although other orientations have been suggested (Arulanandam et al., 1994). The effects of complementary amino acid substitutions in rat CD2 and CD48 provide strong evidence for a model based on the crystal contacts (van der Merwe et al., 1995). The dimensions of the complex formed between CD2 and its ligands are likely to be similar to those of the MHC antigen−T cell receptor complex. For this reason it has been suggested that one of the key functions of CD2 is to separate the plasma membranes of interacting cells at the optimal distance for facile surveillance of occupied MHC molecules by T cell receptors (van der Merwe et al., 1995).

In the present study we have characterized line-width and chemical shift perturbations in a two-dimensional $^{15}N-^{1}H$ heteronuclear single-quantum coherence (HSQC) spectrum of rat CD2d1 during titrations with an unlabeled soluble form of rat CD48. This analysis defines the ligand binding site of rat CD2 and addresses the possibility that the interaction with CD48 is accompanied by conformational changes in the ligand binding domain of CD2. The results allow comparisons of the human and rat CD2 ligand binding sites that provide a basis for understanding ligand- and species-specific recognition at the cell surface by CD2.

MATERIALS AND METHODS

Sample Preparation. A uniformly ^{15}N labeled sample of the N-terminal rat CD2 domain (residues 1−99) was produced in *Escherichia coli* as a glutathione *S*-transferase (GST) fusion protein GST−CD2d1 as described previously (Driscoll et al., 1991). The fusion protein was purified by glutathione agarose affinity chromatography and cleaved with thrombin and the product CD2d1 purified by gel filtration. In order to express the ligand of rat CD2 in a form suitable for solution studies, a stop codon was introduced into a cDNA encoding rat CD48 (Killeen et al., 1988; Wong, 1991) after the codon for Ala193, between domain 2 and the transmembrane domain, by polymerase chain reaction. The mutated cDNA was then subcloned into the pE14 vector for expression in Chinese hamster ovary (CHO) cells using the glutamine synthetase-based gene expression system (Bebbington & Hentschel, 1987; Davis et al., 1990). A high expressing clone was selected, and bulk cultures were established as described previously (Davis et al., 1995b). Soluble rat CD48 (sCD48) was purified using immunoaffinity chromatography and gel filtration. Ultrafiltration was used to concentrate the protein samples into identical buffer (20 mM sodium phosphate, pH 7.0). The extinction coefficients of CD2 domain 1 and sCD48 were determined by amino acid analysis (CD2d1 $\epsilon_{280} = 1170\ M^{-1}\ cm^{-1}$, sCD48 $\epsilon_{280} = 1440\ M^{-1}\ cm^{-1}$), allowing for estimation of relative protein concentrations in different samples by measuring the absorbance at 280 nm.

NMR Spectroscopy. NMR spectroscopy was carried out using a home-built/GE Omega hybrid spectrometer of the Oxford Centre for Molecular Sciences, operating at a ^{1}H frequency of 600 MHz. The spectrometer was operated using a Bruker triple nucleus 5 mm probe head. NMR data were processed and analyzed using the software FELIX version 2.3 (BIOSYM Inc.). In the main, experiments were carried out at 25 °C. 2D and 3D $^{1}H-^{15}N$ heteronuclear spectroscopy was performed using water suppression procedures based on the inclusion of "scrambling" spin lock pulses (Messerle et al., 1989) without additional irradiation of the solvent resonance line. Specifically, 2D $^{1}H-^{15}N$ heteronuclear single-quantum coherence (HSQC) spectroscopy (Norwood et al., 1990; Bax et al., 1990) was used to follow the pH-dependent chemical shifts of the $^{1}H-^{15}N$ cross peaks and to map the CD2d1 interaction surface with sCD48. A single 3D $^{1}H-^{15}N$ NOESY-HSQC experiment (Kay et al., 1989; Messerle et al., 1989) with 150 ms mixing time was recorded for the confirmation of resonance assignments of CD2d1 at pH 7.0. In all cases the NMR data were recorded in such a manner to optimize the baseline flatness and phase characteristics of signals aliased in the indirectly detected dimensions (Bax et al., 1991). Quadrature detection was obtained using States−TPPI phase cycling procedures (Marion et al., 1989b). Prior to Fourier transformation all data were subjected to solvent signal removal by deconvolution

in the directly detected dimension (Marion et al., 1989a). For the 2D HSQC experiments the sweep widths in the ^{1}H and ^{15}N dimensions were 14.5 and 2.0 kHz, respectively. A total of 128 complex t_1 increments of 1024 complex t_2 points were recorded in each experiment, corresponding to acquisition times of 64 and 70 ms, respectively, with between 16 and 118 scans per increment depending on overall signal strength. After data processing the intensity scales of the processed spectra were normalized prior to the estimation of cross peak volumes. For the 3D NOESY−HSQC experiment the recorded data size was 512 complex t_3 × 32 complex t_2 × 128 complex t_1 data points with sweep widths in the F1, F2, and F3 dimensions of 7246, 2000, and 7246 Hz, respectively. Eight transients were recorded per t_1,t_2 increment.

Resonance Assignments. The solution structure determination of CD2d1 was previously performed using the resonance assignments obtained for a uniformly ^{15}N labeled sample maintained at pH 4.3 (Driscoll et al., 1991). For the purposes of the titration of CD2d1 with sCD48 described in this paper, it was necessary to reassign the ^{1}H−^{15}N HSQC spectrum of CD2d1 at pH 7.0. The reassignment at neutral pH was obtained by following the movement of cross peaks in the spectrum as a function of pH. 2D HSQC data sets were recorded using samples of CD2d1 prepared at pH 4.3, 5.0, 5.8, 6.4, 7.0, and 7.4. There was no evidence of any conformational changes in the CD2d1 structure over this pH range. A further check on the integrity of the reassignment of the spectrum was made through a comparison of a 3D ^{1}H−^{15}N NOESY−HSQC spectrum recorded at pH 7.0 with a data set previously recorded at pH 4.3.

CD2d1/sCD48 Titration. The titration of sCD48 with CD2d1 was performed in the following manner. The initial NMR sample (sample A) contained 0.6 mL total volume 0.375 mM CD2d1 in 20 mM sodium phosphate, pH 7.0 (90% H_2O/10% D_2O), and therefore had a molar ratio of 1:0 CD2d1:sCD48. A second NMR sample (sample B) containing 0.6 mL total volume 0.375 mM CD2d1 and 1.1 mM sCD48 was prepared, which therefore had a molar ratio of 1:2.2 CD2d1:sCD48. The buffer composition of both samples was precisely identical as both CD2d1 and sCD48 underwent final stage purification by gel filtration using the same batch of sodium phosphate buffer. A series of 2D ^{1}H−^{15}N HSQC NMR experiments were performed where the concentration of CD2d1 was maintained at a constant 0.375 mM and the sCD48 concentration varied in stepwise increments to give a series of CD2d1:sCD48 molar ratios from 1:0 to 1:2.2. First, 2D ^{15}N−^{1}H HSQC spectra of the A and B sample tubes were recorded. These spectra represent the end points of the titration series. The samples used for recording data for intermediate values of the CD2d1:sCD48 ratio were obtained by simultaneously removing an aliquot from both sample tube A and sample B tube and then transferring the aliquots to the other NMR tube (i.e., from tube A to tube B and *vice versa*). This procedure of simultaneously exchanging equal volume aliquots was repeated until a series of 12 experiments covering the range of CD2d1:sCD48 ratios from 1:0 to 1:2.2 had been completed. Since the initial CD2d1 concentration was the same in samples A and B, the CD2d1 concentration remained constant and only the sCD48 concentration varied throughout the titration series. This was confirmed by performing SDS−PAGE on 5 μL aliquots of the A and B samples extracted at each aliquot exchange. Spectra of CD2d1:sCD48 at 1:1 ratio showed identical spectra over a period of weeks, ruling out very slow conformational changes or aggregation effects.

RESULTS

Protein Expression. The identification of the ligand of rat CD2 as CD48 (van der Merwe et al., 1993a) provided an opportunity to study the ligand interactions of CD2 in solution since the structure of the ligand binding domain of rat CD2 is well characterized by NMR methods (Driscoll et al., 1991). It proved necessary to express a soluble form of the ligand in a eukaryotic expression system because domain 1 of CD48 was insoluble when expressed alone in *E. coli* (D. C. McPherson, S. J. Davis, and A. F. Williams, unpublished data). A construct encoding a soluble form of rat CD48 (sCD48) was therefore prepared for expression in CHO cells using the glutamine synthetase-based gene expression system (Bebbington & Hentschel, 1987; Davis et al., 1990). A new full-length cDNA encoding rat CD48 (Wong, 1991) was used as a template for insertion of a stop codon after Ala193 of the predicted mature protein sequence by polymerase chain reaction. However, the sequence of the cDNA proved to differ from the published sequence (Killeen et al., 1988) at the codons for residues 116 and 118. The protein sequence in this region was Ile-Lys-Asp rather than Thr-Lys-Asn. The two cDNA sequences were isolated from cDNA libraries generated from two different rat strains (Killeen et al., 1988; Wong, 1991), indicating that rat CD48 is polymorphic in this region. The net effect of the sequence variation is that the Asn118 glycosylation is disrupted and so this form of CD48 is likely to have four rather than five N-linked glycans. A CHO cell clone expressing sCD48 at levels in excess of 80 mg/L was generated and the protein purified by affinity chromatography and gel filtration. The predicted molecular mass of the protein component of sCD48 is *ca.* 23 kDa, but due to the heterogeneous glycosylation of the protein, sCD48 runs on SDS−PAGE as multiple bands with apparent molecular mass in the range 30−45 kDa (data not shown).

Reassignment of the ^{15}N−^{1}H CD2d1 HSQC Spectrum at pH 7.0. The solution structure of the N-terminal domain of rat CD2 domain 1 (CD2d1) has previously been determined using protein produced in a bacterial fusion protein expression system (Driscoll et al., 1991). An essentially complete resonance assignment of the ^{1}H and ^{15}N resonances of the NMR spectrum of a uniformly labeled CD2d1 sample was obtained using a combination of 3D ^{1}H−^{15}N heteronuclear, 2D ^{15}N−^{1}H heteronuclear, and 2D ^{1}H−^{1}H homonuclear NMR methods. In the previously reported work the sample was maintained in 20 mM phosphate buffer at pH 4.3. However, because CD2 does not bind to CD48 below *ca.* pH 6, samples for the binding experiments were prepared in buffer at the more physiologically realistic pH 7.0. It was also necessary to reassign the ^{1}H and ^{15}N spectra of CD2d1 at the elevated pH. In order to accomplish this, a series of 2D ^{15}N−^{1}H HSQC experiments were performed over the pH range 3.90−7.4 to track movement of the amide NH cross peaks within the spectra. A 3D NOESY−HSQC experiment recorded at pH 7.0 was used to confirm the assignment of the 2D HSQC spectrum, by analysis of the NOE connectivities in the 3D heteronuclear NMR data recorded previously at pH 4.3 (Driscoll et al., 1991). At the end of this analysis a HSQC cross peak could be assigned unambigu-

ously for 82 of the total 99 residues of CD2d1 at pH 7.0. For remaining residues, six cross peaks are lost due to the increased rate of solvent exchange at the higher pH (Arg1, Asp2, Ser3, Gly4, Ser36, and Gly53), and nine cross peaks could not be unambiguously assigned due to cross peak overlap (Phe23, Arg44, Lys47, Lys51, Ile57, Ala59, Asn84, Arg87, and Leu95). In addition, CD2d1 contains two prolines (Pro19, Pro48) that lack NH groups and therefore do not produce $^{1}H-^{15}N$ HSQC cross peaks. All the asparagine and glutamine side chain NH_2 cross peaks and the two tryptophan residue indole ring NH signals were also reassigned.

Titration of ^{15}N CD2d1 with sCD48. To follow the effects of binding CD48 to CD2 in solution, we performed a series of 12 2D $^{15}N-^{1}H$ HSQC experiments on various mixtures of uniformly ^{15}N-labeled CD2d1 and the soluble form of the extracellular domain of rat CD48, sCD48. The titration was performed in such a manner that the concentration of CD2d1 remained constant throughout and the amount of sCD48 increased from 0 to 2.2 mol equiv. The titration points corresponded to CD2d1:sCD48 molar ratios of 1:0, 1:0.05, 1:0.11, 1:0.22, 1:0.39, 1:0.55, 1:0.77, 1:1.00, 1:1.21, 1:1.48, 1:1.83, and 1:2.20.

A number of different characteristic behaviors of the CD2d1 NH cross peaks could be identified in the course of the titration. Figure 1 shows a small region of the HSQC spectra of mixtures of ^{15}N-CD2d1:sCD48 at three different points through the titration corresponding to molar ratios 1:0, 1:0.2, and 1:1.0. This region can be used to illustrate the various types of behavior identified.

(A) Overall Cross Peak Broadening. There is an overall broadening of cross peaks of the CD2d1 HSQC spectrum with increasing sCD48 concentration, characterized by a general loss of intensity through the spectrum. This is evident from Figure 1C where it is clear that all cross peaks are broader (have lower intensity) than at the lower ratios of sCD48 to CD2d1. At higher ratios of sCD48 to CD2d1 the cross peaks continue to broaden, and at a ratio of CD2d1:sCD48 of 1:2.2 essentially all CD2 NH cross peaks corresponding to ordered polypeptide backbone regions of CD2 have broadened to the noise. A naive interpretation of the overall broadening of the spectrum is that it can be ascribed to an increasing total protein concentration through the titration range, leading to higher solution viscosity. However, that the broadening of the CD2 spectrum is due to binding to CD48 is evidenced by the result that, upon lowering the pH below 6.0, the complete spectrum of the ^{15}N-CD2d1 is regained with all cross peaks showing essentially identical line widths to the spectrum of CD2d1 alone (data not shown). This is in accord with real-time binding measurements showing that the binding of multivalent rat CD48 to rat CD2 is dramatically weakened as the pH falls below 6.0 (van der Merwe et al., unpublished results). These results suggest that a protonation equilibrium on the interaction surface of one or both of CD2 and CD48 is able to modulate the strength of interaction between these two proteins.

(B) The Rates of CD48-Induced Cross Peak Broadening Vary for Different Cross Peaks. Some peaks broaden very rapidly below the noise level at the CD2d1:sCD48 molar ratio of 1:0.77 (Figure 2). For example, in Figure 1 the cross peak of Glu31 has significantly broadened at a CD2d1:sCD48 ratio of 1:0.2 (Figure 1B) and has disappeared from the spectrum at a molar ratio of 1:1.0 (Figure 1C). The cross

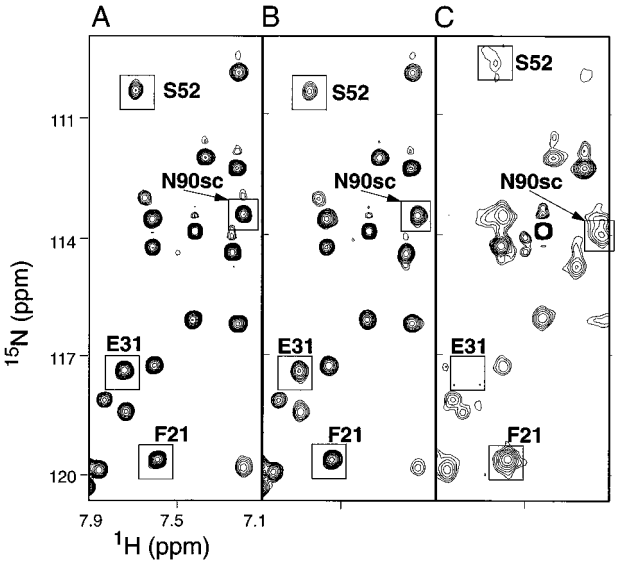

FIGURE 1: A selected region of three 2D $^{15}N-^{1}H$ HSQC spectra of CD2d1 (0.375 mM) is shown in the presence of (A) 1:0, (B) 1:0.2, and (C) 1:1 mol equiv of sCD48. Cross peaks represent the correlation between the ^{15}N and NH resonances of each NH group in CD2d1. Several peaks are labeled to illustrate the different degrees of sCD48-induced changes in chemical shift and peak broadening. Peaks corresponding to the backbone Glu31 broadened rapidly and disappeared before any chemical shift change was observed, while the Ser52 cross peak and the side chain NH_2 cross peak of Asn90 (N90sc) were both significantly displaced. The backbone amide of Phe21 was not displaced at all and broadened slowly in comparison to other peaks.

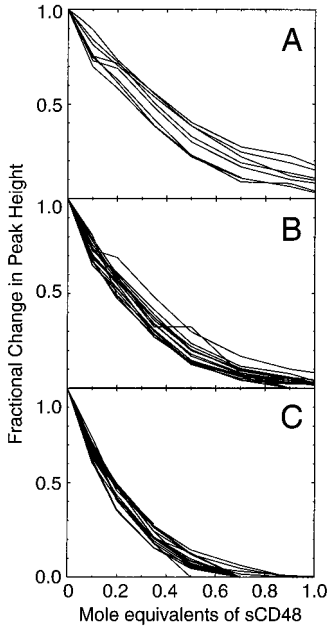

FIGURE 2: The peak heights of all cross peaks that did not shift significantly were measured at each step in the CD2d1−sCD48 titration. The fractional reduction in peak height (Δh) was calculated as follows: $\Delta h = (h_a - h_x)/(h_a - h_b)$, where h_x is the height of a cross peak at one point in the titration, h_a is the initial peak height in the spectrum of CD2d1 alone, and h_b is the peak height at the end of the titration (2.2 mol equiv of sCD48). Δh is plotted against the molar ratio of CD2d1:sCD48. Individual plots for cross peaks that broadened most slowly with increasing sCD48 concentration are superimposed in (A), residues with an intermediate rate of broadening in (B), and cross peaks that are most sensitive to sCD48-induced broadening in (C).

peaks corresponding to the backbone NHs of Phe21 and Ser52 and the NH_2 group of Asn90 broaden less rapidly and

are still visible in panel C of Figure 1. In all, 20 cross peaks had broadened beyond detection by the 1:1.0 step in the titration. Only a small number of cross peaks were still visible at the end of the titration (CD2d1:sCD48 ratio 1:2.2). These signals correspond to highly flexible regions of the CD2d1 structure, including the side chain indole NϵH of Trp9, the backbone amide NH of the C-terminal residue Glu99, and all but two of the pairs of asparagine NH_2 group signals.

The differences in the broadening behavior of the different cross peaks are shown in Figures 2 and 3. Figure 2 shows the plots of the peak intensity versus CD2d1:sCD48 ratio for three different sets of cross peaks corresponding to those signals which broaden more slowly through the titration (Figure 2A), those signals which broaden at an intermediate rate (Figure 2B), and those signals which broaden most rapidly and have essentially disappeared from the spectrum at a CD2d1:sCD48 ratio of 1:1.0 (Figure 2C). Figure 3 shows a histogram of the relative peak heights for all the backbone amide NH signals between the spectrum of CD2d1 on its own and the CD2d1:sCD48 mixture with ratio 1:0.2 (i.e., at a relatively early point in the titration). The histogram shows that the peaks which are more profoundly affected by the presence of sCD48 correspond to regions of the secondary structure of CD2d1 including the C and C′ β-strands, Phe49 of the C″ strand as well as the C-terminal part of the F-strand, the F−G loop, and the N-terminal residue of the G-strand. The least affected peaks come from the B−C and A−B loops, the beginning of the A-strand, and the C-terminal end of the G-strand—all regions which are at the extremities of the domain fold.

(C) A Small Number of Cross Peaks Shift as Well as Broaden. For the majority of cross peaks in the CD2d1 HSQC spectrum the sCD48-induced broadening occurs in the absence of discernible chemical shift changes. However, for a few cross peaks, small sCD48 concentration-dependent changes in ^{1}H and/or ^{15}N chemical shifts can be detected superposed on the overall broadening. This type of behavior is exemplified by the NH peak of Ser52 and the downfield side chain NH_2 peak of Asn90 (Figure 1). The chemical shift changes of the side chain NH_2 cross peaks of Asn90 and Asn77 could be followed throughout the complete course of the titration. While the cross peak definition is rather poorly defined because of a low signal-to-noise ratio at the higher concentrations of sCD48, it appeared that the total chemical shift changes reach a limiting "saturated" level within the titration range of the experiment. This is interpreted to indicate that essentially complete complex formation between CD2 and CD48 is attained by the end of the titration, consistent with a dissociation constant for the complex of the two proteins in the 10−100 μM range**.** The direction and magnitude of the chemical shift changes due to sCD48 binding were dissimilar to any chemical shift changes observed in the pH titration of CD2d1 alone.

sCD48-induced chemical shift changes were measured for all cross peaks in the CD2d1 HSQC spectrum recorded with a CD2d1:sCD48 ratio of 1:1.0. These values are given in histogram form in Figure 4. Individual graphs are given for the change in ^{1}H chemical shift (Figure 4A), change in ^{15}N chemical shift (Figure 4B), and "vector" shift, which combines the changes in ^{1}H and ^{15}N chemical shifts (in hertz) into the length of the vector joining the position of the cross peak positions in the 1:0 and 1:1.0 CD2d1−sCD48 spectra.

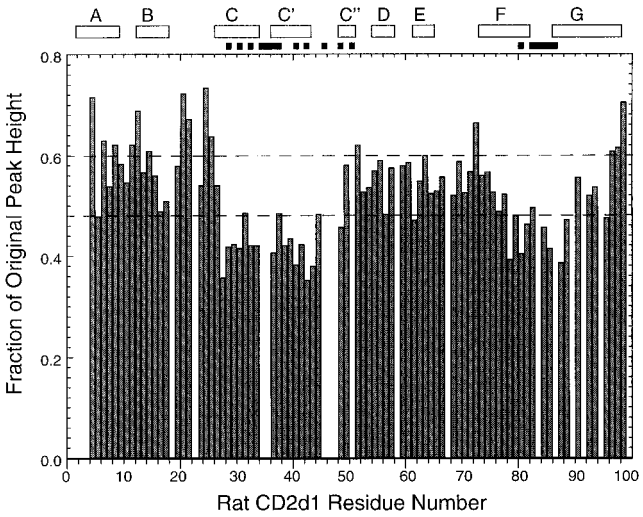

FIGURE 3: Plot of the fractional change in peak height between the spectrum of CD2d1 alone and the spectrum of CD2d1 with 0.2 mol equiv sCD48. The fractional change in peak height was calculated as described in Figure 2. The fractional change in peak height is plotted against CD2d1 residue number to illustrate the difference in the initial rate of sCD48-induced cross peak broadening. The two horizontal dashed lines across the figure represent the boundaries chosen to categorize the different degrees of sCD48-induced cross peak broadening for mapping onto the CD2d1 structure (Figure 5). The absence of a bar indicates that the cross peak either could not be assigned or could not be reliably quantified. The Asn90 cross peak became overlapped with Lys51/Ala59 on titration with sCD48 so that the peak height could not be measured accurately, but appeared to broaden rapidly before becoming overlapped. The positions of the CD2d1 β-strands are depicted at the top of the figure. The residues involved in rat CD2 homodimer interaction in the crystal lattice (Jones et al., 1992) are indicated by black filled boxes (■) at the top of the figure.

Note that for a number of residues the amide NH cross peak has already broadened beyond detection at this point in the titration. These residues are indicated by black bars in Figure 4. Of the remaining residues, most have cross peaks that showed either very small (<10 Hz) or intermediate changes in chemical shift. A small number of cross peaks showed large (>35 Hz) chemical shift changes. This latter group includes the backbone NHs of Trp32, Arg34, Leu38, Glu41, Ser52, Phe55, Leu63, Thr79, and Arg96 along with the side chain amide NH_2 resonances of Asn90.

Comparison of Figures 3 and 4 shows that the majority of the peaks which exhibited large (>35 Hz) CD48-induced shifts were also strongly selectively broadened: i.e., the corresponding peak height in the 1:0.2 CD2d1:sCD48 HSQC spectrum was less than 45% of the original height in the CD2d1 only spectrum. This observation supports the notion that those peaks which were broadened beyond detection in the 1:1.0 CD2d1:sCD48 HSQC spectrum actually experience the largest sCD48-induced peak shifts and therefore should be considered the most strongly perturbed. Again cross peaks with this characteristic correspond to residues in β-strands C, C′, C″, F, and G.

DISCUSSION

Chemical shift perturbation is well established as a powerful probe of ligand binding sites on proteins [reviewed by Otting et al. (1993)]. In particular, random ^{15}N (or ^{13}C) labeling has been commonly used as a means to selectively detect which regions of a protein are involved in the interaction with protein or nonprotein ligands. The chemical

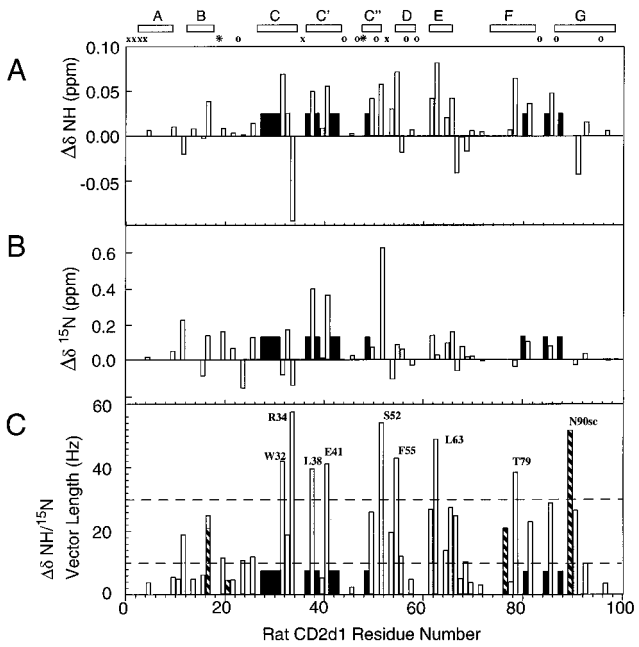

FIGURE 4: Plots of sCD48-induced change in chemical shift ($\Delta\delta$) for the backbone NH proton (A) and ^{15}N resonances (B) versus the CD2d1 amino acid residue number. The chemical shift difference for all assigned cross peaks was measured between the CD2d1 HSQC spectrum and the HSQC spectrum of equimolar CD2d1 and sCD48. The combined ^{15}N/NH chemical shift change, measured as the length of the resultant vectors representing the ^{1}H and ^{15}N chemical shift changes, is shown in (C). Cross peaks that had broadened beyond detection in the 1:1.0 CD2d1−sCD48 spectrum are shown as black bars of uniform height. Chemical shift changes for the side chain NH_2 amide cross peaks of Asn17, Asn77, and Asn90 are indicated by cross-hatched boxes in (C). Residues that were not assigned because of spectral overlap are indicated at the top of the figure by "o" and residues that could not be assigned because of solvent exchange broadening by "x". Proline residues are indicated by "*". The chemical shift change vector was calculated from the square root of the sum of the squared NH and ^{15}N chemical shift differences in hertz. The β-strands are represented by boxes at the top of the figure. The two dashed lines drawn across (C) at 10 and 30 Hz represent the cutoff limits chosen for categorizing the different degrees of chemical shift change for mapping onto the CD2d1 structure (Figure 6).

shifts of both the ^{1}H and ^{15}N nuclei are sensitive to changes in conformation or electronic environment. For example, when two proteins form a complex, changes in the electronic environment at the interface will result in selective chemical shift changes of nuclei in the vicinity. In the absence of evidence for structural perturbations of the labeled component, ligand-induced chemical shifts can be used to map the binding site. The advantage of isotope-labeling one of the components of the complex is that the NMR spectrum is dramatically simplified, and individual cross peaks can be monitored in 2D heteronuclear spectra even when the complex formed has a relatively high molecular weight. Among many other examples this methodology has been used to investigate the binding sites of phosphotyrosine-containing peptides to SH2 domains (Hensman et al., 1994; Rosen et al., 1995), the binding of proline-rich peptides to SH3 domains (Yu et al., 1992; Booker et al., 1993) and profilins (Archer et al., 1994; Metzler et al., 1994), the binding of phosphorylated lipid to a pleckstrin homology domain (Harlan et al., 1994), interactions between protein G and an antibody Fc fragment (Gronenborn & Clore, 1993; Kato et al., 1995), the binding of a peptide fragment of type 1 interleukin-8 receptor to interleukin-8 (Clubb et al., 1994), and mapping the binding interfaces of the histidine-containing protein Hpr and enzyme II in the bacterial phosphotransferase system (van Nuland et al., 1993; Chen et al., 1993). In each of these cases, the ligand-induced spectral changes can be followed throughout the course of ligand addition, so that the chemical shifts of the majority of cross peaks can be observed in the presence of the fully formed complex. The observation of the majority of the cross peaks in the fully formed complex indicates that the rotational correlation time of the complex must be reasonably short, thereby yielding signals with a sufficiently long transverse relaxation time to be observed in the 2D heteronuclear NMR spectra. In contrast, at least two examples of the use of monitoring ^{15}N labels in protein−ligand complex formation have yielded qualitatively dissimilar results. In the cases of the ^{15}N-labeled POU-specific DNA binding domain in complex with a 20mer duplex oligonucleotide (Dekker et al., 1993) and the interaction between the ^{15}N-labeled Ras-binding domain of c-Raf-1 and full-length N-Ras(Asp12)-GMPPNP (Emerson et al., 1995), the effects of the ligand on the protein spectrum included the selective broadening of amide NH cross peaks corresponding to the intermolecular interface region.

In this paper we describe the application of ^{15}N−^{1}H heteronuclear NMR spectroscopy to the interaction between the cell−cell recognition molecules CD2 and CD48. In particular, we followed the changes in the spectrum of ^{15}N-labeled CD2d1 upon addition of up to 2.2 molar equiv of sCD48. The overriding effect observed was the general broadening of the HSQC cross peaks with increasing sCD48 concentration (Figure 1). In general, few significant ligand-induced chemical shift effects were observed, and the most discriminating factor in the behavior of the CD2d1 cross peaks was differential broadening. The behavior of each cross peak in the CD2d1−sCD48 titration HSQC spectra could be described in one of three ways (a) no significant change in chemical shift and relatively slow broadening with increasing sCD48 concentration, (b) significant chemical shift change accompanied by an increased sensitivity to sCD48-induced cross peak broadening, and (c) strong cross peak broadening at relatively low sCD48 concentration and eventual disappearance from the HSQC spectrum at around 1 mol equiv of added sCD48. Figures 5 and 6 show schematic representations of the three-dimensional structure of CD2d1 illustrating the location of residues which exhibited differential cross peak broadening effects (Figure 5) and sCD48-induced changes in cross peak chemical shifts (Figure 6).

The behavior of the CD2d1 HSQC cross peaks in the titration is consistent with a mechanism of intermediate to fast "chemical" exchange on the NMR time scale between free and sCD48-bound CD2d1. The general broadening of the CD2d1 spectrum can be attributed to the averaging of the line widths of the resonances of free CD2d1 and CD2d1 in a complex with sCD48. Because we could not detect the majority of signals at the highest concentrations of sCD48, we assume that this complex has a long rotational correlation time leading to very short transverse relaxation times. Variation of the temperature (up to 45 °C) at which the spectra were recorded had no significant effect on the appearance of the HSQC spectrum.

The differential broadening exhibited by the different amide NH cross peaks can be understood in terms of the

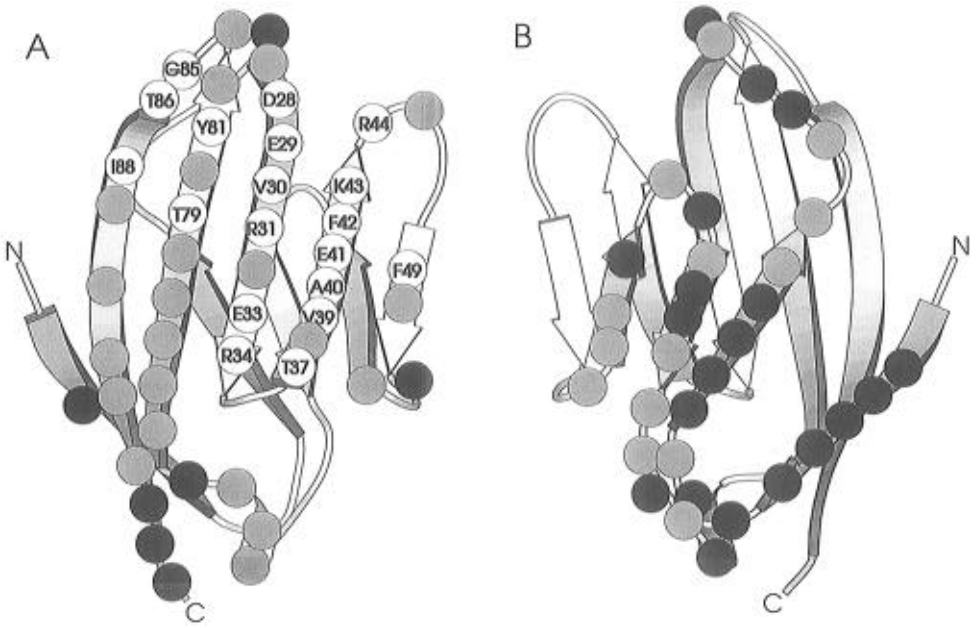

FIGURE 5: Schematic representation of the three-dimensional solution structure of rat CD2 domain 1 showing the differential effects of cross peak broadening in the HSQC spectrum of CD2d1 with 0.2 mol equiv of sCD48 (see Figure 3). In (A) the structure is shown with the major β-sheet facing forward. From left to right the β-strands are named A, G, F, C, C′, and C″. The differential broadening of cross peaks is indicated by the following scheme: residues showing the least sensitivity to sCD48-induced broadening are shown with black circles, residues with intermediate cross peak broadening with gray circles, and residues with the most pronounced cross peak broadening with white circles. In the last category the residue identity is given. (B) uses the same scheme for the CD2d1 structure rotated by 180° about the vertical axis from (A) to illustrate the effects on the minor β-sheet surface, comprising (from left to right) β-strands D, E, and B, together with the N-terminal strand A.

formula for the contribution to the transverse relaxation rate for a resonance undergoing two-site exchange in the fast exchange limit, $R_{2,\mathrm{exch}}$:

$$R_{2,\mathrm{exch}} = p_{\mathrm{complex}}R_{2,\mathrm{complex}} + p_{\mathrm{free}}R_{2,\mathrm{free}} + p_{\mathrm{complex}}p_{\mathrm{free}}\tau(2\pi\Delta\delta)^2$$

where p_{complex} and p_{free} are the mole fractions of the ligand in complexed and free forms, respectively, $R_{2,\mathrm{complex}}$ and $R_{2,\mathrm{free}}$ are the transverse relaxation rates in the complex and free states, $\Delta\delta$ is the difference in chemical shifts between the two forms, and τ is the lifetime of the complex state (Lian et al., 1994). In other words, the line width is a weighted average of the free and bound ligand resonances plus an additional exchange term. Outside the limit of "very fast exchange" ($\tau \rightarrow 0$) and with a finite chemical shift difference $\Delta\delta$ between the bound and free state resonances, the exchange term contributes an additional factor to the line width of the average signal. Thus, the cross peaks which connect resonances which are most strongly shifted in the complex also exhibit the strongest line broadening due to exchange. The application of this formula to the behavior of the amide NH cross peaks in the CD2d1−sCD48 titration indicates that those peaks which show the fastest rate of broadening with respect to increasing sCD48 concentration are those peaks which are subject to the largest chemical shift perturbations. In turn, the corresponding residues are those which represent the center of the CD2d1−sCD48 binding interface.

Figures 5 and 6, which illustrate the major cross peak broadening and chemical shift effects observed in the titration with sCD48, indicate that the most strongly perturbed residues are centered on the upper portion of the major β-sheet surface of CD2d1 (Figures 5A and 6A). The region most strongly affected comprises residues from the complete length of β-strands C and C′, the C-terminal half of strand F, and the N-terminal half of strand G, with peripheral effects on isolated residues in the loop connecting strands C′ and C″ and on strand C′ itself. On the opposing β-sheet face, comprising β-strands B, E, and D, only two significant spectral perturbations are observed, namely, CD48-induced cross peak shifts of the amide NH resonances of Phe55 and Leu63. None of the amides exhibiting the strongest tendency for CD48-induced cross peak broadening are on this side of the CD2 molecule (Figures 5B and 6B).

The side chain amide NH_2 cross peaks of all the asparagine and glutamine residues as well as the side chain indole NH cross peak of Trp7 could be followed throughout the course of the titration, presumably reflecting the intrinsically higher mobility and therefore narrower resonances of these groups. Of these, only the NH_2 cross peaks of Asn77 and Asn90 exhibited chemical shift perturbations and line broadening due to sCD48. The downfield side chain NH_2 cross peak of Asn77 shifted 21 Hz and broadened to an intermediate extent, suggesting that it is likely to be on the edge of the binding site, while the Asn90 side chain NH_2 cross peak underwent a larger chemical shift change (52 Hz) and broadened quite significantly (Figure 1) and is therefore more likely to be closer to the CD48 interaction site. Asn77 is located in the central region of β-strand F and Asn90 is in an adjoining position in β-strand G. In both of these cases the Asn side chains are on the periphery of the sCD48 binding site mapped out by the strongest chemical shift perturbations to backbone amide NH cross peaks. All of the other side chain resonances correspond to residues in regions well removed from this site. Rat CD2 expressed in CHO cells is glycosylated on residue Asn77. The electron density of the *N*-acetylglucosamine residue attached to this residue in the crystal structure of rat CD2 suggests that the

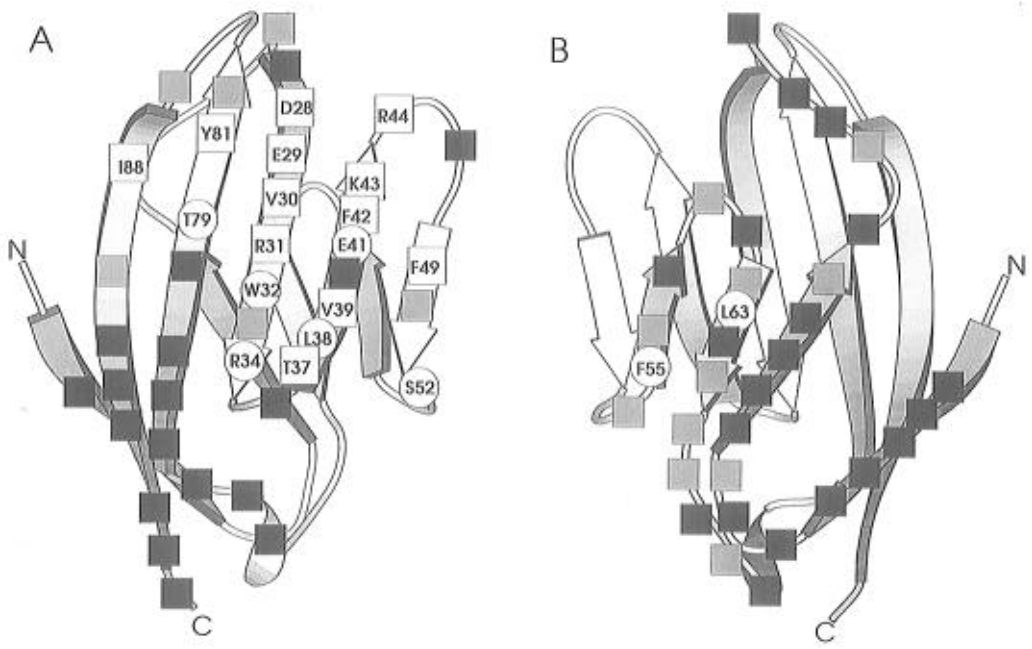

FIGURE 6: Two views of the rat CD2 domain 1 structure, shown in the same orientations as in Figure 5, depicting the distribution of sCD48-induced cross peak shifts. A white circle indicates that the chemical shift difference between the spectrum of CD2d1 alone and a spectrum of equimolar CD2d1 and sCD48 was greater than 30 Hz. A gray square indicates a chemical shift difference of between 10 and 30 Hz, and a black square indicates a chemical shift change smaller than 10 Hz. White circles highlight residues for which the cross peak had broadened beyond detection by this stage of the titration, presumably indicating a high degree of chemical exchange broadening.

oligosaccharide is oriented toward the bottom of β-strands F and G. This is presumed to leave the upper part of the major β-sheet face free to bind CD48, clear from steric hindrance from the N-linked glycan at Asn77 (Jones et al., 1992).

We consider that the most strongly perturbed amide NH cross peaks in our experiment are for residues Asp28, Glu29, Val30, Arg31, Trp32, Glu33, Arg34, Thr37, Leu38, Val39, Ala40, Glu41, Phe42, Lys43, Arg44, Phe49, Thr79, Tyr81, Gly85, Thr86, and Ile88 (see Figures 5 and 6). Of these, Asp28, Glu29, Arg31, Glu33, Thr37, Leu38, Glu41, Lys43, Phe49, Thr79, Tyr81, and Gly85 have side chains which are directed into solution from the major β-sheet face. The others have side chains that are either totally buried in the core of the domain, partially buried under the C−C′ loop (Arg34), or pointing away from the face of the domain (Arg44, Thr86, and Ile88). Figure 7A shows a representation of the three-dimensional fold of CD2d1 and highlights the position of the amide protons that are implicated by the NMR titration data as the binding surface for sCD48.

Mutagenesis studies have identified some of the residues involved in the interaction of human CD2 with its ligand CD58 (Arulanandam et al., 1993; Peterson & Seed, 1987; Somoza et al., 1993; Wolff, 1990). Sixteen residues in total were identified as being involved in the interaction. These residues are mostly charged (10 charged, 4 hydrophobic, and 2 polar) and map onto the human CD2 G, F, C, C′, and C″ β-strands and the F−G, C−C′ and C′−C″ loops. For the residues at homologous positions in the rat CD2 sequence nine had backbone NH cross peaks which were strongly broadened in the presence of sCD48 (Glu29, Arg31, Glu33, Glu41, Arg43, Tyr81, Gly85, Thr86, Ile88), and Leu38 had a cross peak which exhibited intermediate broadening but a large (>30 Hz) chemical shift change. Of the remainder, Ser82 showed an intermediate cross peak shift (10−30 Hz) with an intermediate degree of broadening, Met46, Asn77, and Asn90 were essentially unperturbed, and the cross peaks of the remaining three residues could not be assigned because of peak overlap or solvent exchange broadening. The surface region of rat CD2d1 that experiences the greatest perturbation upon sCD48 binding therefore corresponds well with the positions of the human CD2 residues identified as important for binding human CD58. Of the 12 residues that make up the surface binding patch identified in the NMR study, 5 are conserved in human CD2 (Asp28, Glu33, Phe49, Tyr81, Gly85), 4 are conservatively substituted (Glu29, Arg31, Lys43, and Thr79 are replaced in human CD2 by Asp, Lys, Arg, and Ser residues, respectively), and 3 have charge changes (Thr37, Leu38, and Glu41 are replaced in human CD2 by Lys, Lys, and Gln, respectively). Figure 7C,D shows a color-coded representation of the amino acid character (acidic, basic, polar, and hydrophobic) for residues in this surface patch on the rat CD2d1 and human CD2d1 structures, respectively. Rat CD2 does not interact with sheep or human CD58 (Somoza et al., 1993), and human CD2 does not bind rat CD48 (P. A. van der Merwe and S. J. Davis, unpublished data). It is conceivable that residues 37, 38, and 41 play a major role in determining the ligand and species specificity of CD2.

The residues that are buried at the interface of the head-to-head interaction seen in the rat sCD2 crystal lattice (Jones et al., 1992) correspond well to the most strongly perturbed resonances in the CD2d1−sCD48 titration (Figure 7A,B). Of the 18 CD2 residues forming the lattice contact, 13 have significantly perturbed resonances in the presence of CD48 (Figure 3). Amide NH cross peaks could not be assigned for four of the remaining residues, and the Asn90 cross peak overlapped with other peaks. Residues Phe49, Tyr81, and Gly85 are conserved in all CD2 homologues sequenced to date (Tavernor et al., 1994) and are each involved in head-to-head crystal contacts seen in the rat sCD2 and human sCD2 crystals (Jones et al., 1992; Bodian et al., 1994).

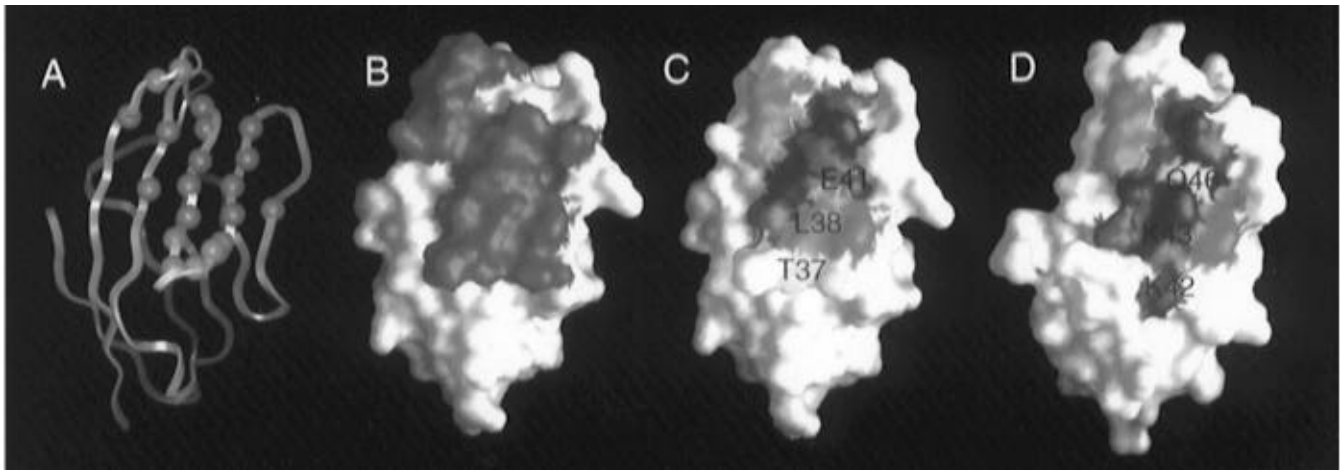

FIGURE 7: (A) Ribbon diagram of the three-dimensional fold of rat CD2d1. Blue spheres indicate the location of the amide nitrogen atoms of the 21 residues that experience the strongest sCD48-induced perturbations in the NMR spectrum. (B) Representation of the molecular surface of rat CD2d1. The surface is colored red for the 18 exposed residues that make up the head-to-head lattice contact in the crystals of rat CD2. (C and D) Amino acid character of the side chains that comprise the ligand binding patches of rat CD2 and human CD2, respectively, using data from this NMR study and previously reported mutagenesis studies, respectively. Acidic residues are colored red, basic residues blue, hydrophobic residues green, and polar residues yellow. The three side chains with different character between the two binding patches are indicated: Thr37, Leu38, and Glu41 in (C) and Lys42, Lys43, and Gln46 in (D), respectively. (A) was made with the program InsightII (BIOSYM Inc.) and (B−D) were created using the program GRASP (Nicholls et al., 1991). In (B−D) the orientation of the protein structure is as in (A).

Nonconservative mutation of these residues disrupts the binding of human CD2 to CD58 or the interaction of rat CD2 with CD48 (Peterson & Seed, 1987; Davis et al., unpublished results). It was suggested that these residues might be directly involved in ligand binding (Bodian et al., 1994), and this is consistent with the observation that the backbone amide NH resonances of all three residues were significantly perturbed in the presence of sCD48. Main chain H-bonds in the vicinity of residues 38 and 85 (rat CD2 numbering) were an additional conserved feature of the lattice contacts in the rat and human CD2 crystals. While ligand-induced peak broadening of the Gly85 backbone amide and the large change in the backbone amide chemical shift of Leu38 implicate these residues in binding, additional work will be required to confirm that these effects are due to the formation of main chain H-bonds with sCD48. There is, however, a remarkable concordance between the surface patch of rat CD2d1 implicated in the binding of sCD48 and that involved in the rat sCD2 crystal lattice dimer contact (Figure 7A,B). Since it is likely that CD2 and its ligand evolved from a common ancestor with homophilic adhesion properties (Wong et al., 1990), it is expected that the interaction observed in the crystal lattice may mimic the interaction of CD2 with its ligand *in vivo*. Good evidence for this model of the interaction has previously been obtained by the real-time binding analysis of the effects of complementary mutations on the major β-sheet surfaces of rat CD2 and CD48 (van der Merwe et al., 1995).

Human T lymphocyte activation and the binding of certain ligand-blocking antibodies to domain 1 of CD2 induce the appearance of a neoepitope on domain 2 of CD2 (Meuer et al., 1984). Moreover, the addition of certain combinations of domain 1 and 2 binding antibodies to T lymphocytes *in vitro* causes cell activation (Meuer et al., 1984). A comparable phenomenon occurs with CD2 monoclonal antibodies and rat T lymphocytes (Clark et al., 1988). Conformational changes in CD2 were among the first mechanisms invoked to explain the induction of the neoepitope (Meuer et al., 1984), and this concept remains popular (Bagnasco et al., 1993; Rouleau et al., 1994). However, in the light of the three-dimensional structure of the whole extracellular region of CD2 (Jones et al., 1992; Bodian et al., 1994), it is difficult to envisage the transmission of conformational changes from domain 1 to domain 2. Such a mechanism is also inconsistent with the locations of the epitopes of activating anti-rat CD2 and anti-human CD2 antibodies (Davis et al., 1995a). In this study we find no evidence of any disruption of the overall secondary structure of CD2d1 upon binding sCD48. None of a subset of NH cross peaks corresponding to core residues bear signs of chemical shift perturbation including, for example, the internally hydrogen-bonded indole NH of Trp32 in the domain core.

In summary, we have investigated the interaction in solution of domain 1 of rat CD2 with its physiological ligand CD48 using NMR spectroscopy. The CD48 binding region of CD2 has been mapped by following the distribution of differential sCD48-induced cross peak broadening and chemical shift changes. This study maps the interaction site to the upper region of the major β-sheet surface, including β-strands C, C′, C″, F, and G, with a surface area that matches the nonphysiological lattice contact in the crystal structure of rat CD2 (*ca.* 700−800 Å^2). Comparative analysis of the human and rat CD2 ligand binding sites suggests that as few as three residues, Thr37, Leu38, and Glu41, could be responsible for the species-specific ligand binding characteristics of CD2.

ACKNOWLEDGMENT

P.C.D. acknowledges Dr. Bruno Kieffer of the University of Strasbourg for valuable discussions. We thank Dr. A. Neil Barclay for a critical reading of the manuscript.

REFERENCES

Archer, S. J., Vinson, V. K., Pollard, T. D., & Torchia, D. A. (1994) *FEBS Lett. 337*, 145−151.

Arulanandam, A. R. N., Withka, J. M., Wyss, D. F., Wagner, G., Kister, A., Pallai, P., Recny, M. A., & Reinherz, E. L. (1993) *Proc. Natl. Acad. Sci. U.S.A. 90*, 11613−11617.

Arulanandam, A. R. N., Kister, A., McGregor, M. J., Wyss, D. F., Wagner, G., & Reinherz, E. L. (1994) *J. Exp. Med. 180*, 1861−1871.
Bagnasco, M., Franco, M.-D., Lopez, M., Nunes, J., Lipcey, C., Mawas, C., Salamero, J., & Olive, D. (1993) *Hum. Immunol. 38*, 172−178.
Bax, A., Ikura, M., Kay, L. E., Torchia, D. A., & Tschudin, R. (1990) *J. Magn. Reson. 86*, 304−318.
Bax, A., Ikura, M., Kay, L. E., & Zhu, G. (1991*) J. Magn. Reson. 91*, 174−178.
Bebbington, C. R., & Hentschel, C. C. G. (1987) in *DNA Cloning: A Practical Approach* (Glover, D. M., Ed.) Vol. III, pp 163−188, IRL Press, Oxford.
Beyers, A. D., Spruyt, L. L., & Williams, A. F. (1992) *Proc. Natl. Acad. Sci. U.S.A. 89*, 2945−2949.
Bierer, B. E., Sleckman, B. P., Ratnofsky, S. E., & Burakoff, S. J. (1989*) Annu. Rev. Immunol. 7*, 579−599.
Bodian, D. L., Jones, E. Y., Harlos, K. H., Stuart, D. I., & Davis, S. J. (1994) *Structure 2*, 755−766.
Booker, G. W., Gout, I., Downing, A. K., Driscoll, P. C., Boyd, J., Waterfield, M. D., & Campbell, I. D. (1993) *Cell 73*, 813−822.
Bork, P., Holm, L., & Sander, C. (1994) *J. Mol. Biol. 242*, 309−320.
Chen, Y., Reizer, J., Saier, M. H., Fairweather, W. J., & Wright, P. (1993) *Biochemistry 32*, 32−37.
Clark, S. J., Law, D. A., Paterson, D. J., Puklavec, M., & Williams, A. F. (1988) *J. Exp. Med. 167*, 1861−1872.
Clubb, R. T., Omichinski, J. G., Clore, G. M., & Gronenborn, A. N. (1994) *FEBS Lett. 338*, 93−97.
Davis, S. J., Ward, H. A., Puklavec, M. J., Willis, A. C., & Williams, A. F. (1990) *J. Biol. Chem. 265*, 10410−10418.
Davis, S. J., Davies, E. A., & van der Merwe, P. A. (1995a) *Biochem. Soc. Trans. 23*, 188−194.
Davis, S. J., Davies, E. J, Barclay, A. N., Daenke, S., Bodian, D. L., Jones, E. Y., Stuart, D. I., Butters, T. D., Dwek, R. A., & van der Merwe, P. A. (1995b) *J. Biol. Chem. 270*, 369−375.
Dekker, N., Cox, M., Boelens, R., Verrijzer, C. P., van der Vliet, P. C., & Kaptein, R. (1993) *Nature 362*, 852−855.
Driscoll, P. C., Cyster, J. G., Campbell, I. D., & Williams, A. F. (1991) *Nature 353*, 762−765.
Dustin, M. L., & Springer, T. A. (1991) *Annu. Rev. Immunol. 9*, 27−66.
Emerson, S. D., Madison, V. S., Palermo, R. E., Waugh, D. S., Scheffler, J. E., Tsao, K.-L., Keifer, S. E., Liu, S. P., & Fry, D. C. (1995) *Biochemistry 34*, 6911−6918.
Gronenborn, A. M., & Clore, G. M. (1993) *J. Mol. Biol. 233*, 331−335.
Harlan, J. E., Hajduk, P. J., Yoon, H. S., & Fesik, S. W. (1994) *Nature 371*, 168−170.
Hensmann, M., Booker, G. W., Panayotou, G., Boyd, J., Linacre, J., Waterfield, M., & Campbell, I. D. (1994) *Protein Sci. 3*, 1020−1030.
Hunig, T. (1985) *J. Exp. Med. 162*, 890−901.
Jones, E. Y., Davis, S. J., Williams, A. F., Harlos, K., & Stuart, D. I. (1992) *Nature 360*, 232−239.
Kato, K., Koyanagi, M., Okada, H., Takanashi, T., Wong, Y. W., Williams, A. F., Okumura, K., & Yagati, H. (1992) *J. Exp. Med. 176*, 1241−1249.
Kato, K., Lian, L.-Y., Barsukov, I. L., Derrick, J. P., Kim, H.-H., Tanaka, R., Yoshino, A., Shiraishi, M., Shimada, I., Arata, Y., & Roberts, G. C. K. (1995) *Structure 3*, 79−85.
Kay, L. E., Marion, D., & Bax, A. (1989) *J. Magn. Reson. 84*, 72−84.
Killeen, N., Moessner, R., Arvieux, J., Willis, A., & Williams, A. F. (1988) *EMBO J. 7*, 3087−3091.
Lian, L. Y., Barsukov, I. L., Sutcliffe, M. J., Sze, K. H., & Roberts, G. C. K. (1994) *Methods Enzymol. 239*, 657−700.
Marion, D., Ikura, M., & Bax, A. (1989a) *J. Magn. Reson. 84*, 425−430.
Marion, D., Ikura, M., Tschudin, R., & Bax, A. (1989b) *J. Magn. Reson. 85*, 393−399.
Messerle, B. A., Wider, G., Otting, G., Weber, C., & Wuthrich, K. (1989) *J. Magn. Reson. 85*, 608−613.
Metzler, W. J., Bell, A. J., Ernst, E., Lavoie, T. B., & Mueller, L. (1994) *J. Biol. Chem. 269*, 4620−4625.
Meuer, S. C., Hussey, R. E., Fabbi, M., Fox, D., Acuto, O., Fitzgerald, K. A., Hodgdon, J. C., Protentis, J. P., Schlossman, S. F., & Rheinherz, E. L. (1984) *Cell 36*, 897−906.
Moingeon, P., Chang, H. C., Sayre, P. H., Clayton, L. K., Alcover, A., Gardner, P., & Rheinherz, E. L. (1989) *Immunol. Rev. 111*, 111−144.
Nicholls, A., Sharp, K. A., & Honig, B. (1991) *Proteins 11*, 281−296.
Norwood, T. J., Boyd, J., Heritage, J. E., Soffe, N., & Campbell, I. D. (1990*) J. Magn. Reson. 87*, 488−501.
Otting, G. (1993) *Curr. Opin. Struct. Biol. 3*, 760−768.
Peterson, A., & Seed, B. (1987) *Nature 329*, 842−846.
Recny, M. A., Luther, M. A., Knoppers, M. H., Neidhardt, E. A., Khandekar, S. S., Concino, M. F., Schimke, P. A., Francis, M. A., Moebius, U., Reinhold, B. B., Reinhold, V. N., & Reinherz, E. L. (1992) *J. Biol. Chem. 267*, 22428−22434.
Rosen, M. K., Yamazaki, T., Gish, G. D., Kay, C. M., Pawson, T., & Kay, L. E. (1995) *Nature 347*, 477−479.
Rouleau, M., Mollereau, B., Bernard, A., Metivier, D., Rosenthal-Allieri, M. A., Charpentier, B., & Senik, A. (1994) *J. Immunol. 152*, 4861−4872.
Selvaraj, P., Plunkett, M. L., Dustin, M. L., Sanders, M. E., Shaw, S., & Springer, T. A. (1987) *Nature 326*, 400−403.
Somoza, C., Driscoll, P. C., Cyster, J. G., & Williams, A. F. (1993) *J. Exp. Med. 178*, 549−558.
Spruyt, L. L., Glennie, M. J., Beyers, A. D., & Williams, A. F. (1991) *J. Exp. Med. 174*, 1407−1415.
Tavernor, A. S., Kydd, J. H., Bodian, D. L., Jones, E. Y., Stuart, D. I., Davis, S. J., & Butcher, G. W. (1994) *Eur. J. Biochem. 219*, 969−976.
van der Merwe, P. A., McPherson, D. C., Brown, M. H., Barclay, A. N., Cyster, J. G., Williams, A. F., & Davis, S. J. (1993a) *Eur. J. Immunol. 23*, 1373−1377.
van der Merwe, P. A., Brown, M. H., Davis, S. J., & Barclay, A. N. (1993b) *EMBO J. 12*, 4945−4954.
van der Merwe, P. A., Brown, M. H., Davis, S. J., & Barclay, A. N (1993c) *Biochem. Soc. Trans. 21*, 340S.
van der Merwe, P. A., Barclay, A. N., Mason, D. W., Davies, E. A., Morgan, B. P., Tone, M., Krishnam, A. K. C., Ianelli, C., & Davis, S. J. (1994) *Biochemistry 33*, 10149−10160.
van der Merwe, P. A., McNamee, P. N., Davies, E. A., Barclay, A. N., & Davis, S. J. (1995) *Curr. Biol. 5*, 74−84.
van Nuland, N. A. J., Kronn, G. J. A., Dijkstra, K., Wolters, G. K., Scheek, R. M., & Robillard, G. T. (1993) *FEBS Lett. 315*, 11−15.
Williams, A. F., & Barclay, A. N. (1988) *Annu. Rev. Immunol. 6*, 381−405.
Williams, A. F., Barclay, A. N., Clark, S. J., Paterson, D. J., & Willis, A. C. (1987) *J. Exp. Med. 165*, 368−380.
Withka, J. M., Wyss, D. F., Wagner, G., Arulanandam, A. R. N., Reinherz, E. L., & Recny, M. A. (1993) *Structure 1*, 69−81.
Wolff, H. L., Burakoff, S. J., & Bierer, B. E. (1990) *J. Immunol. 144*, 1215−1220.
Wong, Y.-W. (1991) D. Phil. Thesis, Oxford University.
Wong, Y.-W., Williams, A. F., Kingsmore, S. F., & Seldin, M. F. (1990*) J. Exp. Med. 171*, 2115−2130.
Wyss, D. F., Choi, J. S., Li, J., Knoppers, M. H., Willis, K. J., Arulanandam, A. R. N., Smolyar, A., Reinherz, E. L., & Wagner, G. (1995) *Science 269*, 1273−1278.
Yu, H., Rosen, M. K., Shin, T. B., Seidel-Dugan, C., Brugge, J. S., & Schreiber, S. L. (1992) *Science 258*, 1665−1667.

BI952756U